Australian Journal of Basic and Applied Sciences, 9(12) Special 2015, Pages: 128-133

ISSN:1991-8178

Australian Journal of Basic and Applied Sciences

Journal home page: www.ajbasweb.com

Annealing Temperature Effects on Morphological and Optical Studies of Nano and Micro Photonics Lithium Niobate using for Optical Waveguide Applications

[1,2]Makram. A. Fakhri, [3]Y. Al-Douri, [4]Uda. Hashim,[5] Evan. T. Salim

[1,3,4]Institute of Nano Electronic Engineering (INEE), University Malaysia Perlis (UniMAP), Perlis, Malaysia
[2]Laser and Optoelectronic department, University of technology, Baghdad .Iraq
[5]Laser science branch, University of technology, Baghdad. Iraq

ARTICLE INFO

Article history:
Received 22 February 2015
Accepted 20 March 2015
Available online 25 April 2015

Keywords:
LiNbO3 thin film, optical properties, structure properties, photonic applications

ABSTRACT

Lithium niobate (LiNbO3) nano and micro structures are deposit on glass substrate by sol-gel method. The nanostructures are deposited by spin coating at 3000 rpm for 30 sec and annealed at 400, 500, 600, 700 oC respectively. They are characterized and analyzed by Atomic Force Microscopy and Ultre-Violet visible. The measurements results show that at increasing of molarity concentration, the structures start to crystallize to become more regular distribution

© 2015 AENSI Publisher All rights reserved.

To Cite This Article: Makram. A. Fakhri, Y. Al-Douri, Uda. Hashim, Evan. T. Salim., Annealing Temperature Effects on Morphological and Optical Studies of Nano and Micro Photonics Lithium Niobate using for Optical Waveguide Applications. ***Aust. J. Basic & Appl. Sci., 9(12): 128-133, 2015***

INTRODUCTION

Lithium niobate (LiNbO3) is an important ferroelectric materialand it has become a very attractive material for integrated optical applications because of its excellent piezoelectrical, electrooptical, pyroelectrical, photo-refractive properties, acousto-optical and nonlinear optical devices properties (S. Grilli,2006), (E. Marenna *et al*., 2009). Lithium niobate (LiNbO3) is a widely used polar material for photonic applications (P. Kumar *et al*.,2010), (Jian Zhang, and Xinping Zhang, 2014). It is employed in nonlinear optics for frequency conversion and in telecommunication for electro-optic modulation (Liang Cao *et al*. 2014), (Hongyun Chen *et al*, 2013). It is a very attractive material for the fabrication of optical wave-guide devices (Pranabendu Ganguly *et al*., 2012), (Abd El–Naser A *et al*., 2011). From experimental estimation, a direct and indirect energy band gap of LiNbO3 is reported to be in the range of 3.5 - 4.7 eV basing on LiNb3) concentrations. These changes are attributed to several parameters like grain size, composition and defects (S. Mamoun *et al*., 2013), (C. Thierfelder *at al*., 2010), (A. Tumuluri *et al*., 2014). There are a lot of work has been devoted to fabricate LiNbO3 thin films,by various experimental techniques like sputtering (O. P. Nautiyal and S. C. Bhatt, 2011) sol-gel process (L. H. Wang *et al*.,2007), liquid phase epitaxy (LPE) (k. peithmann *et al*., 2006), metal organic chemical vapor deposition (MOCVD) (Kazumi Kato *et al*., 2009), soft- chemistry (Maëlenn Aufray *et al*., 2009), hydrothermal methods (Gaku Isobe *et al*., 2011), and pulsed laser deposition (PLD) (Xinchang Wang *et al*, 2013). LiNbO3 is a widely used polar material for photonic applications (X. Wang,2005), (P.Ganguly, 2012). It is employed in nonlinear optics for frequency conversion, telecommunication for electro-optic modulation (H. Lu *et al*., 2012) and fabrication of optical wave-guide devices (Abd El–Naser A *et al*. 2011), (K. S. Kaur *et al*, 2011) and Surface acoustic wave device (SAW) (H.K. Lam *et al*., 2004). LiNbO3 waveguides are already widely used in many functional electro-optic and acoustooptic devices (H. Chen *et al*. 2013) Waveguide structures are essential for many integrated-optic devices.

This work reports the preparation of LiNbO3 nanostructures by utilizing the spin-coating technique. The characterization and analysis have been elaborated as a function of molarity concentration. The refractive index is the main work on optical waveguides for LiNbO3 because of refraction coefficients between the base and deposit samples will ensures access to total internal reflection that give us better realizing of optical

Corresponding Author: Makram. A. Fakhri, Institute of Nano Electronic Engineering (INEE), University Malaysia Perlis (UniMAP), Perlis, Malaysia

waveguide. The refractive index is measured and calculated to fit best application of optical waveguide , then we prepared the thin film and enhanced it to get a high quality film have an optical properties exactly like single crystal LiNbO3 wafers .

Experiment process:

The preparation procedure for $LiNbO_3$ films by using Nb_2O_5 (ultra-purity, 99.99%), and cetric acid (CA.) are used without further purification. The solution is prepared by mixing Li_2CO_3, Nb_2O_5, citric acid and Ethylene Glycol. The molar ratio between Li_2Co_3 and Nb_2O_5 was 1:1 in order to maximize the formation of $LiNbO_3$ stoichiometry phase. Firstly, the $LiCo_3$, Nb_2O_5, and citric acid were dissolved in Ethylene Glycol with heating and stirring at 90 C for 48 hours, then mixed all together with continue heating and stirring at 90 C for 48 hour. To obtain homogeneous and crack-free films of $LiNbO_3$,the precursor were deposited by spin coating technique on glass substrates at a spinning speed of 3000 rpm for 30 sac. Seven layers were prepared, the film was dried at 120 ^{O}C for 5 min and calcined at 2500 ^{O}C for 30 min in static air and oxygen atmosphere to remove the organics then it was annealing at 400, 500, 600, 700 ^{O}C respectively . The thickness of the annealed samples was studied using Scanning Optical Reflectometer model (Filmetrics F20, China). The Atmoic Force Microscopy (AFM) (SPM-9600, Scanning Probe Microscope, Shimadzu, Japan) for investigating the roughness of $LiNbO_3$. The optical properties were investigated using the double-beam Ultr-Violet (UV-vis) spectrophotometer (Shimadzu UV-Vis 1800, Japan)

RESULTS AND DISCUSSION

Morphological studies:

The grain size and root meant square could be affected by Annealing temperatures. Figure 1 shows AFM images of the $LiNbO_3$ nanostructures with a uniform dense surface and exhibits a increase in grain size with increasing the annealing temperatures. The surface topography of $LiNbO_3$ nanostructures as observed from the AFM micrographs proves that the grains are uniformly distributed within the scanning area (5 µm x 5 µm), with individual columnar grains extending upwards. This surface characteristic is important from the topographic images that found at 500 ^{O}C to be uniform, smooth and homogeneous than others.

In association with the increase of the average diameter of grain size from **64.327** to **167.539** nm, Small grains appear on the lower annealing temperature (Fig. 1a). On the other hand, we note that the surface roughness decrease with annealing temperature increases because of the particles be increased results effects of temperature on it , so they roughness is ranging between 10.6-16.0 nm.

The thickness was determined using an optical reflectometer. In the same time, the thickness of film decrees with increasing the annealing temperatures, which leads to increase the deposition process and number of atoms as shown in Fig.2. The increasing of is followed by increasing of the annealing temperatures affect positively on the size of grain that guide to tarnished the surface to become more smooth.

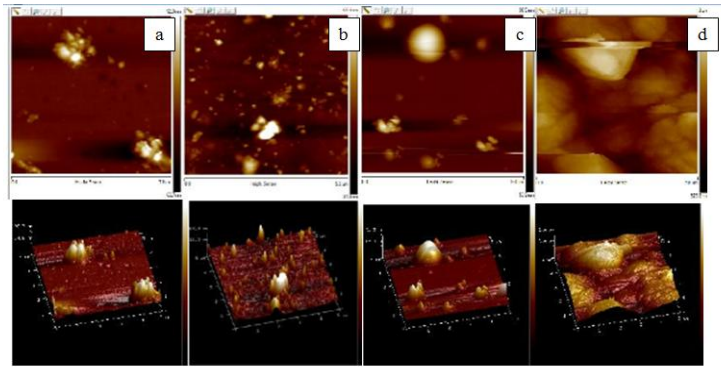

Fig. 1: AFM images of $LiNbO_3$ nanostructures at different annealing temperature (a) 400 ^{O}C , (b) 500 ^{O}C, (c) 600 ^{O}C and (d) 700 ^{O}C.

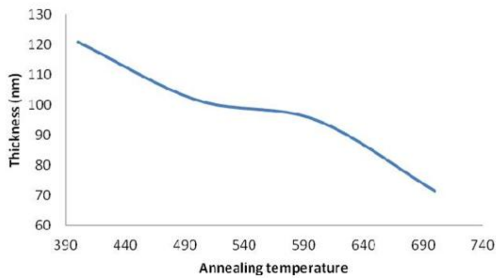

Fig. 2: Thickness of $LiNbO_3$ nanostructures at room temperature.

Optical properties:

The transmission spectra of $LiNbO_3$ nanostructures at different annealing temperature is shown in Fig. 3a, it was found that the transmission increase as annealing temperature increases due to increasing the grain size and decreasing in structure thickness. These values of transmission are about 89.25 – 95.99% with annealing temperature (400 700) ^oC. The deposited samples were white to brown in color and show high transmittance; this is due to excessive $LiNbO_3$ atoms in the structure (I.-K. Jeong *et al*., 2011). The high value of transmittance is attributed to these excessive (LiNbO3) ions existing at interstitial sites that probably transparent for light.

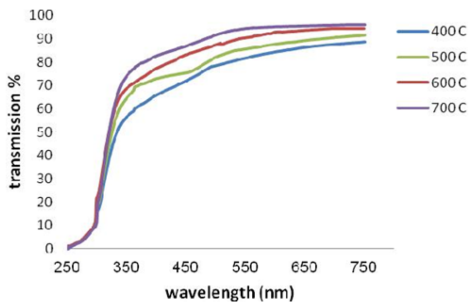

Fig. 3a: Transmission spectra of $LiNbO_3$ nanostructures in different molar concentrations.

The wide direct band gap makes $LiNbO_3$ good material for potential applications in optoelectronic and photonic devices such as multilayer dielectric filters, optical waveguides, SAW and solar cell due to decreasing the window absorption loses and that will improves the short circuit current of the cell. The energy band gap (Eg) is found by plot $(\alpha h\nu)^2$ vs hν as shown in Fig. 3b, as given in Table 2 with good accordance with experimental value (E.T. Salim *et al*., 2014)

Table 1: The energy band gaps, refractive index and optical dielectric constant correspond to moalrity concentration of $LiNbO_3$ nanostructures.

Annealing temperature	E_g (eV)	E_g (eV) Exp (N.S.L.S. Vasconcelos *et al* .,2003)	*n*	*n* Exp (David E. Zelmon and D. L. Small , 1997)	*T*%	Grean size (nm)
400	4.2	2.66 - 4.22 eV	2.43	2.4272	89.26	64.327
500	4		2.47		92.33	88.912
600	3.85		2.52		94.23	102.714
700	3.6		2.54		95.99	167.539

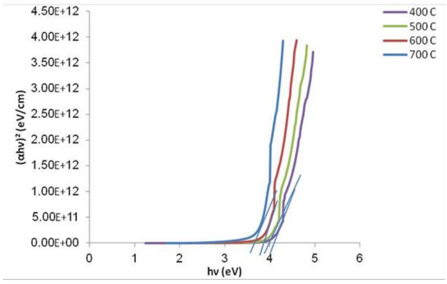

Fig. 2b: Energy band gap of $LiNbO_3$ nanostructures in different molar concentrations.

The optical reflectance (R%) of $LiNbO_3$ nanostructures was measured using double-beam UV-vis and it can be calculated from the absorption and the transmittance spectrum using the relation; R+T+A = 1. Figure 3c shows the reflectance of $LiNbO_3$ nanostructures in the wavelength range 250-800 nm at room temperature.

The refractive index (*n*) was determined from a transmittance spectrum as a function of the wavelength in the range 250-700 nm. The *n* can be determined from the transmission spectrum. There is a decreasing in the refractive index in the visible range; it was estimated 2.43 – 2.54 at 330 nm as shown in Fig. 3d and given in Table 2. The refractive index changes slightly and steadily after 330 nm to 800 nm (T.GHOSH *et al*., 2012), (D.L. Zhang *et al*. ,2014) as given in Table 2. We can notice from that the refractive index increases as annealing temperature increases. This behavior may be attributed to increasing of grain size and decreasing of thickness as a result of the annealing temperature. All the highest values of refractive index is a suitable for optical waveguide.

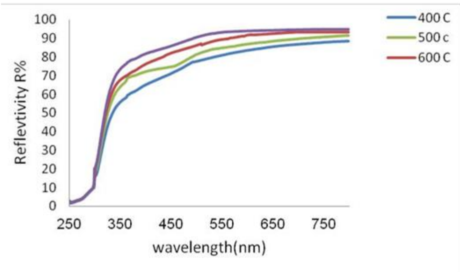

Fig. 3c: Reflection spectra of $LiNbO_3$ nanostructures in different molar concentrations.

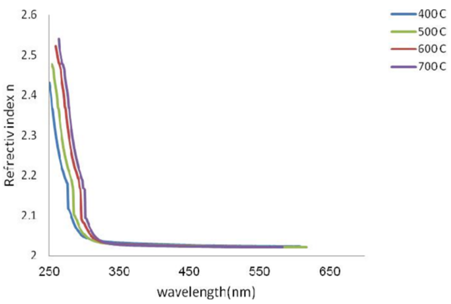

Fig. 3d: Refractive index of $LiNbO_3$ nanostructures in different molar concentration.

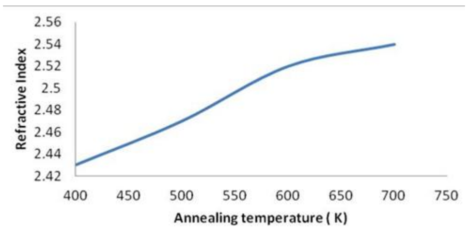

Fig. 3e: Refractive index with concentration of $LiNbO_3$ nanostructures in different annealing temperature

Figre 3e shows the relationship between *n* and the molality concentration that justifies the direct correlation between *n* and M to big grain size affects directly on the refractive index.

Conclusion:

The $LiNbO_3$ nanostructures have been chemically prepared by spin-coating technique. AFM shows diameter of gain size (from 64 to 167) nm, and roughness ranging between 10.6-16.0 nm. Optical properties give high values of transmission that is about 89 - 96% and the measured energy band gaps are 3.6, 3.85, 4, 4.2 eV, We found an approximate match between the energy band gap in the values calculated using the transmission. Refractive index is determined from the transmission spectrum and found that the highest value is an appropriate for optical waveguide.

REFERENCES

Abd El–Naser, A., Mohamed, Mohamed, A. Metawe'e, Ahmed Nabih Zaki Rashed , Amira I. M. Bendary, 2011. Ultra High Speed Semiconductor Electrooptic Modulator Devices for Gigahertz Operation in Optical Communication Systems. International Journal of Optics and Applications, 2011, 1(1) : 1-7

A. Tumuluri, K.L. Naidu, K.C. James Raju (2014). Band gap determination using Tauc's plot for LiNbO3 thin films . International Journal of ChemTech Research CODEN (USA): IJCRGG, 6 : 3353-3356

C. Thierfelder, S. Sanna, A. Schindlmayr, W. G. Schmidt (2010). Do we know the band gap of lithium niobate?. Phys. Status Solid (C), 7(2): 362–365

David E. Zelmon and D. L. Small (1997). Infrared corrected Sellmeier coefficients for congruently grown lithium niobate and 5 mol. % magnesium oxide–doped lithium niobate. J. Opt. Soc. Am. B, 14: 3319-3322

D.L. Zhang, Q. Zhang, C.X. Qiu, W.H. Wong, E. Y. B. Pun, 2014. Zr4+ diffusion-doping effect on refractive index of LiNbO3: A comparison with bulk-doping case, Optical Mnterials Exoress, 4: 2215-2220

E. Marenna, C.Aruta, E.rFanelli, M.Barra , P.Pernice, A.Aronne, 2009. Sol–gel synthesis of nanocomposite materials based on lithium niobate nanocrystals dispersed in a silica glass matrix. Journal of Solid State Chemistry, 182: 1229-1234.

Salim, E.T., Y. Al-Douri, M.S. Al Wazny, M.A. Fakhri, 2014. Optical properties of Cauliflower-like Bi2O3 nanostructures by reactive pulsed laser deposition (PLD) technique . Solar Energy, 107: 523–529.

Gaku Isobe, Peter Bornmann, Tobias Hemsel, Takeshi Morita, 2011. High temperature tolerant transducer for Ultrasonic Assisted Hydrothermal Method "Proceedings of Symposium on Ultrasonic Electronics, 32: 19-20.

Chen, H., T. Lv, A. Zheng, Y. Han, 2013. Discrete diffraction based on electro-optic effect in periodically poled lithium niobate. Optics Communications, 294: 202–207.

Lam, H.K., J.Y. Dai, H.L.W. Chan, 2004. Orientation controllable deposition of LiNbO3 films on sapphire and diamond substrates for surface acoustic wave device application. Journal of Crystal Growth, 268: 144–148.

Lu, H., B. Sadani, G. Ulliac, N. Courjal, C. Guyot, J.M. Merolla, M. Collet, F.I. Baida and M.P. Bernal, 2012. 6-micron interaction length electro-optic modulation based on lithium niobate photonic crystal cavity, Optics Express, 20: 20884-20893.

Hongyun Chen, Tao Lv, Anshou Zheng, Yanling Han, 2013. Discrete diffraction based on electro-optic effect in periodically poled lithium niobate . Optics Communications, 294(1): 202–207.

Jeong, I.K. 2011. Correlated Thermal Motion in Ferroelectric LiNbO3 Studied Using Neutron Total Scattering and a Rietveld Analysis . Journal of the Korean Physical Society, 59: 2756-2759.

Jian Zhang, Xinping Zhang, 2014. Biomolecular binding dynamics in sensors based on metallic photonic crystals. Optics Communications, 320(1): 56-59.

Kazumi Kato, Tadashi Takenaka, Masasuke Takata and Kazuo Shinozaki, 2009. Preparation of Epitaxial $LiNbO_3$ Thin Film by MOCVD and its Properties. Key Engineering Materials, 388 : 179-182

Peithmann, K., M.R. Zamani-Meymian, M. haaks, K. Maier, B. Andreas, K. buse, H. Modrow, 2006. Fabrication of embedded waveguides in lithium-niobate crystals by radiation damage . Appl. Phys. B, 82: 419-422.

Kaur, K.S., A.Z. Subramanian, Y.J. Ying, D.P. Banks, M. Feinaeugle, P. Horak, V. Apostolopoulos, C.L. Sones, S. Mailis, R.W. Eason, 2011. Waveguide mode filters fabricated using laserinduced forward transfer . Optics Express , 19 : 9814-9819

Liang Cao, Abdelsalam Aboketaf, Zihao Wang, Stefan Preble, 2014. Hybrid amorphous silicon (a-Si:H)– $LiNbO_3$ electro-optic modulator . Optics Communications,330(1) : 40–44

Wang, L.H., D.R. Yuan, X.L. Duan, X.Q. Wang, and F.P. Yu, 2007. Synthesis and characterization of fine lithium niobate powders by sol- gel method . Cryst. Res. Technol, 42(4): 321-324.

Maëlenn Aufray, Stéphane Menue, Yves Fort, Julien Eschbach, Didier Rouxel, Brice Vincent, 2009. New Synthesis of Nanosized Niobium Oxides and Lithium Niobate Particles and Their Characterization by XPS Analysis. Journal of Nanoscience and Nanotechnology, 9: 4780-4785

Vasconcelos, N.S.L.S., J.S. Vasconcelos, V. Bouquet, S.M. Zanetti, E.R. Leite, E. Longo, L.E.B. Soledade, F.M. Pontes, M. Guilloux-Viry, A. Perrin, M.I. Bernardi, J.A. Varela, 2003. Epitaxial growth of LiNbO thin films in a microwave oven . Thin Solid Films, 436: 213-219.

Nautiyal1, O.P., S.C. Bhatt, 2011. Preparation and Characterization of Lithium Doped Silver Niobate Perovskite System ,American Journal of Materials Science, 1(1): 1-4 DOI: 10. 5923/j.materials.20110101.01.

Ganguly, P., 2012. Semi-analytical analysis of lithium niobate photonic wires Optics Communications, 285: 4347-4352.

Kumar, P., S.M. Babu, S. Perero, R.M.L. Sai, I. Bhaumik, S. Ganesamoorthy and A.K. Karnal, 2010. X-ray photoelectron spectroscopy, high-resolution X-ray direction and refractive index analyses of Ti-doped lithium niobate (Ti:LiNbO3) nonlinear optical single crystal . Pramana, J. Phys., 75(5): 1035-1040

Pranabendu Ganguly, 2012. Semi-analytical analysis of lithium niobate photonic wires Optics Communications, 285(1): 4347-4352.

Grilli, S., 2006. .*Ferroelectric domain engineering and characterization for photonic applications* . Ph.D Thesis, Department of Physics, Royal Institute of Technology, Stockholm, Sweden

Mamoun, S., A.E. Merad, L. Guilbert, 2013. Energy band gap and optical properties of lithium niobate from ab initio calculations. Computational Materials Science, 79: 125-131

Ghosh, T., B. Samanta, P.C. Jana, P. Ganguly, 2012. Determination of Refractive Index Profile and Mode Index from the Measured Mode Profile of Single-Mode LiNbO3-Diffused Waveguides. Fiber and Integrated Optics, 31: 1-10.

Xinchang Wang, Yu Liang, Sifang Tian, Weidong Man, Jianfeng Jia, 2013. Oxygen pressure dependent growth of pulsed laser deposited LiNbO3 films on diamond for surface acoustic wave device application. Journal of Crystal Growth, 375: 73–77

Wang, X., Z. Ye, G. Wu, L. Cao, B. Zhao, 2005. Growth of textured LiNbO3 thin film on Si (111) substrate by pulsed laser deposition . Materials Letters, 59: 2994-2997.